Visualization in Medicine and Life Sciences (2013)
L. Linsen, H. -C. Hege, and B. Hamann (Editors)

Towards Automatic Extraction of the Myocardium in Temporal MRI Using Object-based Segmentation

Teodora Chitiboi[1,2], Anja Hennemuth[1], Lars Linsen[2], Horst Hahn[1,2]

[1] Fraunhofer MEVIS, Bremen, Germany
[2] Jacobs University, Bremen, Germany

Abstract

Visualizing the deformation of the myocardium over an entire heart cycle is essential for the assessment of local defects in the heart muscle. For this purpose, an automatic segmentation of the myocardium is a key requirement, which would then also form the basis for inspecting cardiac morphology, function and perfusion. In this paper we present an automatic object-based approach for segmenting the left ventricle (LV). The algorithm uses prior knowledge about the topology and geometry of the segmented structure, which is integrated in a region-based graph representation of the image. Our method was tested on cine MR sequences with promising results, and it also performed well when applied to perfusion data.

1. Introduction

Cardiovascular disease is the leading cause of death in the Western countries. Out of the various medical imaging techniques, temporal MRI is the reference modality for understanding the beating heart, providing essential information such as morphology, blood flow, perfusion, and tissue properties. Heart function can be assessed by measuring the change in blood volume or ejection fraction (EF) and myocardial wall thickness of the two ventricles in short-axis view. The LV is especially important as it is responsible for supplying oxygenated blood to the entire body.

Visualizing the evolution of the myocardium over several cardiac cycles and highlighting tissue properties such as perfusion can provide valuable information to clinicians, assisting in the diagnosis of various heart conditions and treatment follow-ups. However visualizing the LV myocardium is challenging due to the fact that it is surrounded by structures with similar intensity (liver, right ventricular (RV) myocardium), meaning that standard transfer functions or isolines can not directly solve the task. Thus a dedicated segmentation of the myocardium is an essential, non-trivial step. One problem in particular is that the inner border (endocardium) does not necessarily correspond to the strongest boundary between the myocardium and the blood pool because of the presence of papillary muscles and trabeculations or partial volume effects. For this reason contour-based segmentation approaches that do not use context information often fail. Moreover, the outer border (epicardium) may be indistinguishable from the liver, while fatty tissue surrounding the heart also tend to burden the task.

Although some commercial solutions exist for segmenting the myocardium in cine data (Phillips, Siemens), they are insufficiently reliable for medical practice. Moreover, the popular software products do not offer an automatic segmentation for cardiac perfusion data. Thus clinicians still rely on slice-wise manual segmentation, a tedious task which requires about 20 minutes per patient [PD11] and is subjected to inter-observer variability.

In this work we propose an object-based segmentation method for the LV that uses context information. The novelty of the approach is the grouping of pixels into atomic regions described by a set of properties regarding their intensity, shape and relation to other image regions. The advantages are that image regions are less sensible to noise and give the possibility to directly use local context to infer the myocardial border where it is not directly visible. This approach enables the segmentation of 2-D short axis cine MR data with the goal of tracking of the myocardium over time. At the same time it can be applied to maximum intensity projection (MIP) perfusion data, which shows the same structure, only is usually much more noisy.

© The Eurographics Association 2013.

DOI: 10.2312/PE.VMLS.VMLS2013.013-017

delivered by EUROGRAPHICS DIGITAL LIBRARY www.eg.org diglib.eg.org

2. Related Work

A comprehensive survey of the work on automatic myocardium segmentation was documented by Petitjean et al. [PD11]. The attempts cover a variety of segmentation methods. The entire image needs not be processed since automatic methods exist for detecting a region of interest (ROI) around the heart [CNS*04], which use the temporal variations caused by the moving organ followed by object detection, commonly based on the Hough transform [YTL92]. Pixel-based classification approaches by simple thresholding [KPK06], or more advanced methods such as finding a Gaussian mixture model on the image histogram [PKM*06, KPM*09] or k-means clustering [LGW06], are very sensible to noise, intensity variability due to different scanners and sequences, and turbulence present in the bloodpool. Active appearance models [ÜFS*03, ZPSD10] have to deal with the very high patient and image variability, and require a very large amount of training data. Many approaches try to directly find the myocardial contours using deformable models/active contours on image gradient [GVKS*93, GGCV95], gradient vector flow (GVF) [SPM*03], or level sets [LGW08]. However, these methods face difficulties for low contrast images and are susceptible to local minima or, on the contrary, find strongest borders that do not correspond to the myocardium. Other approaches use a combination of methods such as an initial pixel classification followed by active contours [Jol06] or transform the image in polar coordinates [LCC*10], each having their own limitations with respect to image sharpness. In conclusion, there has been a lot of work towards an automatic segmentation of the myocardium but the problem has not yet been completely solved to deal with the variety of images used in clinical routine.

3. Automatic LV Segmentation

The main source of problems for myocardium segmentation approaches is the lack of contrast between the heart muscle and surrounding structures. We tackle this challenge by employing object-based image analysis on individual 2D slices to roughly label regions that belong to the bloodpool and myocardium using local context information. Our automatic segmentation algorithm for the LV consists of three parts: 1) heart localization, 2) object-based detection and 3) contour refinement.

3.1. Heart Localization

Since the heart is the only moving organ in the image sequence, we can use this information to determine a smaller ROI that will be further processed. To avoid manually choosing the systolic and end-diastolic phases to compare the minimum and maximum heart positions, one can instead consider the pixel variance over time for a given slice I:

$$var(I) = \sum_t (avg_t(I) - I_t)^2$$

where $avg_t(I)$ is the average image over time. This is especially helpful for image sequences that stretch over more than one heart cycle. The resulting image highlights the space occupied by the moving heart, as shown in Figure 1b. An approximate mask is then computed by Otsu thresholding [Ots79] followed by morphological operations (opening and closing) and hole filling. Considering the minimum bounding box of this mask shown in Figure 2a, a seed point s is determined close to the center of the LV using the Hough transform [YTL92]. For contrast enhancement, the sub-image is processed using a sigmoid filter that highlights the mid-range intensities where myocardium is expected, while smoothly cutting off the extreme values.

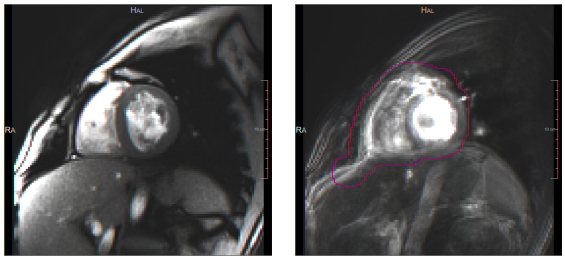

(a) (b)

Figure 1: (a) Initial image; (b) Temporal variance image and ROI.

3.2. Object-based Detection

The idea behind object-based image analysis (OBIA) is to overcome the limitations of pixel-based processing by analyzing image regions in their local semantic context. The image is initially partitioned into regions about 50mm^2 in size, using a k-means clustering algorithm in spatial and spectral dimensions called SLIC super-pixels [ASS*10], which compromises between the region's homogeneity and adherence to borders. The atomic image regions (now called objects) are managed using a generic framework introduced by Homeyer et al. [HSH10] which allows the design of specific object-based segmentation algorithms (e.g. [SMP11, SCHH13]). The objects form a relational graph and are described by a set of properties regarding their shape, orientation, intensity statistics and relative position. In the OBIA image representation one can employ prior information in the form of geometrical (the LV has an elliptical shape) and topological constraints (the bloodpool is surrounded by the myocardium). Starting with the highly over-segmented image, shown in Figure 2b, pairs of adjacent objects are successively merged in a greedy fashion based on their intensity and shape properties to obtain the LV bloodpool and myocardium.

The bloodpool is first roughly estimated by region growing on the super-pixel level, starting from the seed object o_s that contains s. Neighboring objects are successively added as long as their median intensity value is brighter than an adaptive threshold $t_0 = f(I(o_s))$, where $I(o_s)$ is the median

© The Eurographics Association 2013.

intensity of the seed object. Determining an absolute threshold is not possible because of the significant intensity variations per patient but also during a single heart cycle. Thus a threshold function $f = 0.5x + 0.05$ was empirically determined by linear regression over a set of manually chosen region growing thresholds on sample data for given values of $I(o_s)$. The threshold is then iteratively updated using the median intensity of the newly constructed bloodpool region b_i: $t_{i+1} = f(I(b_i))$ and the region growing process is restarted from the initial seed o_s. This is repeated several times until the set of super-pixels forming the bloodpool becomes stable ($b_i = b_{i-1}$). The result is shown in Figure 2c.

Based on the known approximate shape of the bloodpool, a best fitting ellipse with the same area is computed using principal component analysis (PCA), and all neighboring super-pixels which are covered more than 50% are merged. This way the dark papillary muscles are included in the bloodpool and can later be separated by thresholding (Figure 2d). Further small neighboring super-pixels, ordered by their ellipse coverage, are successively added in order to decrease the contour length over area of the resulting bloodpool region, thus improving the compactness of the segmented object.

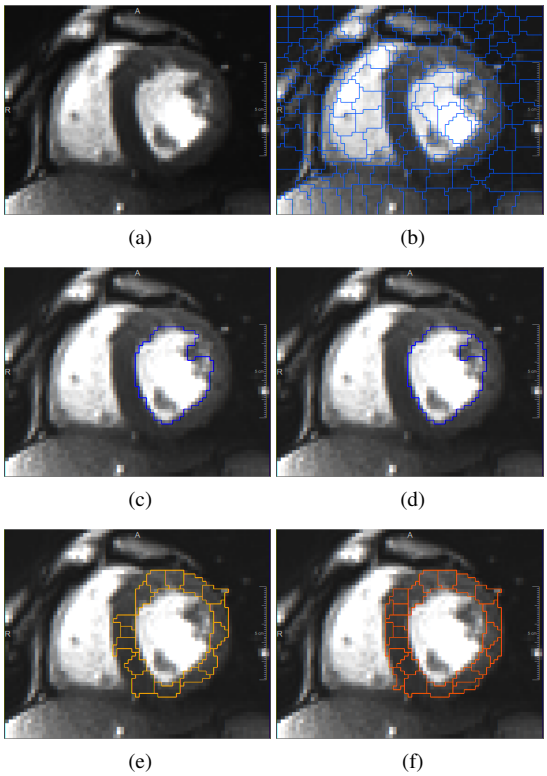

(a) (b) (c) (d) (e) (f)

Figure 2: (a) Original sub-image; (b) Initial super-pixels; (c) Bloodpool - region growing; (d) Bloodpool - ellipse fitting; (e) Initialization myocardium; (f) Identified myocardium super-pixels.

Dictated by the topological constraint, the myocardium is initialized with the first ring of super-pixels surrounding the bloodpool, as shown in Figure 2e. Analyzing the spectral statistics of this new region, we compute the average values $\bar{l}$ and $\bar{u}$ and standard deviations dl and du for the lower and upper quartiles l and u of the preliminary myocardial fragments. Further neighboring super-pixels p' with similar lower and upper quartiles l' and u' are considered in a subsequent region growing step iff. $\bar{l} - 2dl < l'$ and $u' < \bar{u} + 2du$. A super-pixel p' neighboring a myocardium super-pixel p is also classified as part of the myocardium iff. $|avg(p) - avg(p')| < 0.004$ where avg represents the average intensity of the super-pixel normalized to $[0,1]$. This local measure (based on an empirically determined threshold) accounts for significant intensity differences that can appear in certain areas of the myocardium and could not be handled by a global threshold. Possible leakage into the nearby liver is counteracted by restricting the myocardium thickness between 0.7 and 3 cm, which could be further adjusted by medical experience. The expected width is computed per temporal slice according to the heart phase, assuming that the myocardial wall thickness is inversely proportional to the size of the bloodpool. Finally, the joint myocardium-bloodpool mask is also processed by ellipse overlap and a minimal contour constraint, enabling the inclusion of darker super-pixels that fall under the expected endocardial border (Figure 2f).

3.3. Contour Refinement

The object-based segmentation result displays the coarse edges of the original super-pixels. Therefore, the contour is further refined using the active contour algorithm introduced by Kass et al. [KWT88]. The external forces are provided by the anisotropic filtering of the gradient image using the method by Sato et al. [SNS*98], which enhances borders and reduces noise (Figure 3a). The internal forces (tension and stiffness) were balanced empirically to obtain a smooth contour while still following the visible edges. After a fixed number of 300 iterations the final result obtained is showed in Figure 3b.

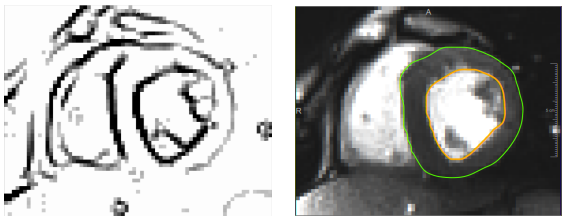

(a) (b)

Figure 3: (a) External forces (inverted gradient); (b) Active contour result.

4. Results and Discussion

The automatic myocardium segmentation algorithm was applied to cine MRI data with promising preliminary results,

© The Eurographics Association 2013.

as shown in Figure 4 - top. Each time point from several medial and upper slices in short-axis view was individually segmented. The segmentation result can be used to visualize the evolution of the myocardium over a cardiac cycle as shown in Figure 6a, and to extract further clinical parameters such as the ejection fraction, blood volume and wall thickness which are essential for diagnosis.

Applying our automatic segmentation algorithm to MIP perfusion data, as shown in Figure 4 - middle, shows its potential to handle noisy data. One application that can be build upon the myocardium segmentation is to determine underperfused myocardial regions by examining the local contrast agent concentration over time. Following specific perfusion segmentation approaches [HSF*08] one can detect the diseased tissue and compare it to the relevant stenosis present on the corresponding coronary artery branch (Figure 5).

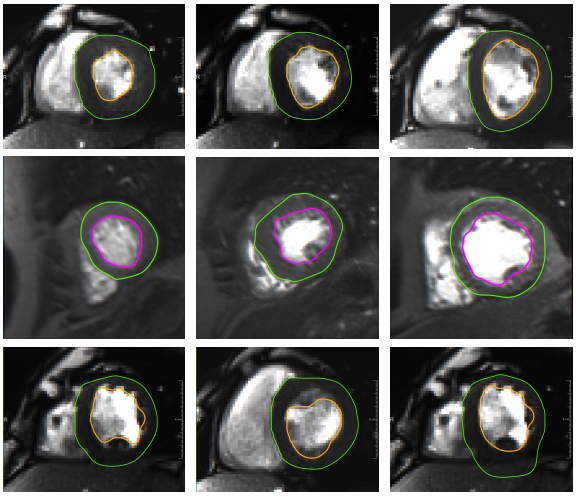

Figure 4: Top: cine MRI segmentation; Middle: MIP perfusion data segmentation; Bottom: limitation are papillary muscles very close to the myocardial wall and no contrast between myocardium and liver.

However some typical segmentation errors may occur (Figure 4 bottom), such as the inclusion of liver tissue in the myocardium in areas where the contrast between the two neighboring anatomical structures is virtually non-existent. The limitations of active contours affect the endocardial border when severe partial volume effects are present or when papillary muscles are pressed against the endocardial wall and show no contrast with the myocardium.

5. Conclusion and Future Work

We have presented an automatic object-based segmentation algorithm for detecting the LV myocardium. OBIA gives us the opportunity to easily formulate and apply prior knowledge such as geometrical and topological constraints, as well as to use local context on a super-pixel level. Both these advantages enable us to correctly detect the myocardial wall

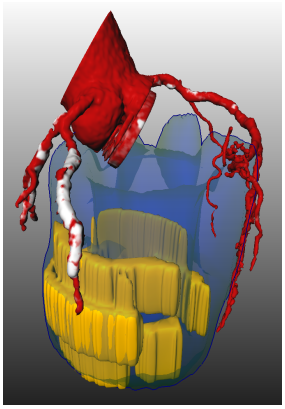

5: 3D visualization of diseased coronary artery branches with stenosis in white, and perfusion segmentation (yellow) obtained on the basis of our automatic myocardium segmentation (blue).

in difficult and noisy settings. The method was tested on short-axis cine MRI data, as well as MIP perfusion data with promising results.

In the future we plan to integrate time coherence information into the segmentation process and insure a smooth transition between the myocardium boundaries in consecutive slices. This can be achieved by checking region overlap in adjacent time points to include or exclude stray regions belonging to the myocardium. Furthermore, a wrong segmentation can be excluded and replaced by propagating the myocardium contours from neighboring time points using, for example, a general registration method as proposed by Tautz et al. [THA*10]. After having assessed the potential of OBIA for object detection in cardiac data, we plan to expand the scope of our algorithm to the entire image scene, also segmenting the RV. Moreover, detecting the lung-liver and RV-liver boundaries, may be helpful in deducing the myocardium-liver boundary where no contrast is available. Figure 6b shows our preliminary progress in this direction. We aim to achieve a successful segmentation of the myocardium in every time point, which will allow for a better inspection of the contractile motion of the LV, and is a crucial step in the extraction and visualization of other myocardial tissue parameters.

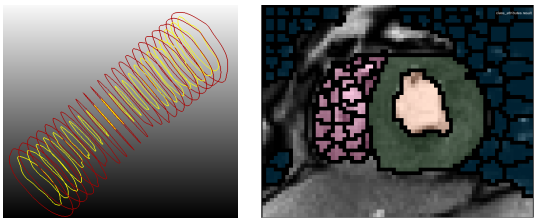

(a) (b)

Figure 6: (a) 3D myocardial contours over time; (b) Object-based detection of the LV bloodpool (yellow) and myocardium (green), RV super-pixels (pink), and lung/air (blue) in cine MRI.

© The Eurographics Association 2013.

References

[ASS*10] ACHANTA R., SHAJI A., SMITH K., LUCCHI A., FUA P., SÜSSTRUNK S.: Slic superpixels. *École Polytechnique Fédéral de Lausssanne, Tech. Rep 149300* (2010). 2

[CNS*04] COCOSCO C. A., NETSCH T., SÉNÉGAS J., BYSTROV D., NIESSEN W. J., VIERGEVER M. A.: Automatic cardiac region-of-interest computation in cine 3d structural mri. In *International Congress Series* (2004), vol. 1268, Elsevier, pp. 1126–1131. 2

[GGCV95] GEIGER D., GUPTA A., COSTA L. A., VLONTZOS J.: Dynamic programming for detecting, tracking, and matching deformable contours. *IEEE Trans. Pattern Anal. Mach. Intell. 17*, 3 (1995), 294–302. 2

[GVKS*93] GUPTA A., VON KUROWSKI L., SINGH A., GEIGER D., LIANG C.-C., CHIU M.-Y., ADLER L., HAACKE M., WILSON D.: Cardiac mr image segmentation using deformable models. In *Proc. Computers in Cardiology* (1993), IEEE, pp. 747–750. 2

[HSF*08] HENNEMUTH A., SEEGER A., FRIMAN O., MILLER S., KLUMPP B., OELTZE S., PEITGEN H.-O.: A comprehensive approach to the analysis of contrast enhanced cardiac mr images. *IEEE Trans. Med. Imag. 27*, 11 (2008), 1592–1610. 4

[HSH10] HOMEYER A., SCHWIER M., HAHN H.: A Generic Concept for Object-based Image Analysis. In *VISAPP* (2010), vol. 2, pp. 530–533. 2

[Jol06] JOLLY M.-P.: Automatic segmentation of the left ventricle in cardiac mr and ct images. *IJCV 70*, 2 (2006), 151–163. 2

[KPK06] KATOUZIAN A., PRAKASH A., KONOFAGOU E.: A new automated technique for left-and right-ventricular segmentation in magnetic resonance imaging. In *EMBS* (2006), IEEE, pp. 3074–3077. 2

[KPM*09] KURKURE U., PEDNEKAR A., MUTHUPILLAI R., FLAMM S. D., KAKADIARIS I. A.: Localization and segmentation of left ventricle in cardiac cine-mr images. *IEEE Trans. Biomed. Eng. 56*, 5 (2009), 1360–1370. 2

[KWT88] KASS M., WITKIN A., TERZOPOULOS D.: Snakes: Active Contour models. *IJCV 1*, 4 (1988), 321–331. 3

[LCC*10] LEE H.-Y., CODELLA N. C., CHAM M. D., WEINSAFT J. W., WANG Y.: Automatic left ventricle segmentation using iterative thresholding and an active contour model with adaptation on short-axis cardiac mri. *IEEE Trans. Biomed. Eng. 57*, 4 (2010), 905–913. 2

[LGW06] LYNCH M., GHITA O., WHELAN P. F.: Automatic segmentation of the left ventricle cavity and myocardium in mri data. *Computers in biology and medicine 36*, 4 (2006), 389–407. 2

[LGW08] LYNCH M., GHITA O., WHELAN P. F.: Segmentation of the left ventricle of the heart in 3-d+ t mri data using an optimized nonrigid temporal model. *IEEE Trans. Med. Imag. 27*, 2 (2008), 195–203. 2

[Ots79] OTSU N.: A threshold selection method from gray-level histograms. *IEEE Trans. Syst., Man, Cybern., Syst. 9*, 1 (jan. 1979), 62 –66. 2

[PD11] PETITJEAN C., DACHER J.-N.: A review of segmentation methods in short axis cardiac mr images. *Med. Image Anal. 15*, 2 (2011), 169–184. 1, 2

[PKM*06] PEDNEKAR A., KURKURE U., MUTHUPILLAI R., FLAMM S., KAKADIARIS I. A.: Automated left ventricular segmentation in cardiac mri. *IEEE Trans. Biomed. Eng. 53*, 7 (2006), 1425–1428. 2

[SCHH13] SCHWIER M., CHITIBOI T., HÜLNHAGEN T., HAHN H.: Automated spine and vertebrae detection and in ct and images. *International Journal for Numerical Methods in Biomedical Engineering in print* (2013). 2

[SMP11] SCHWIER M., MOLTZ J. H., PEITGEN H.-O.: Object-based analysis of CT images for automatic detection and segmentation of hypodense liver lesions. *International Journal of Computer Assisted Radiology and Surgery 6*, 6 (Nov 2011), 737–747. 2

[SNS*98] SATO Y., NAKAJIMA S., SHIRAGA N., ATSUMI H., YOSHIDA S., KOLLER T., GERIG G., KIKINIS R.: Three-dimensional multi-scale line filter for segmentation and visualization of curvilinear structures in medical images. *Med. Image Anal. 2*, 2 (1998), 143 – 168. 3

[SPM*03] SANTARELLI M., POSITANO V., MICHELASSI C., LOMBARDI M., LANDINI L., ET AL.: Automated cardiac mr image segmentation: theory and measurement evaluation. *Med. Eng. & Phys. 25*, 2 (2003), 149. 2

[THA*10] TAUTZ L., HENNEMUTH A., ANDERSSON M., SEEGER A., KNUTSSON H., FRIMAN O.: Phase-based Non-rigid Registration of Myocardial Perfusion MR Image Sequences. In *IEEE ISBI* (2010), pp. 516 – 519. 4

[ÜFS*03] ÜZÜMCÜ M., FRANGI A., SONKA M., REIBER J., LELIEVELDT B.: Ica vs. pca active appearance models: Application to cardiac mr segmentation. *MICCAI* (2003), 451–458. 2

[YTL92] YIP R., TAM P., LEUNG D.: Modification of hough transform for circles and ellipses detection using a 2-dimensional array. *Pattern Rec. 25*, 9 (1992), 1007–1022. 2

[ZPSD10] ZHU Y., PAPADEMETRIS X., SINUSAS A. J., DUNCAN J. S.: Segmentation of the left ventricle from cardiac mr images using a subject-specific dynamical model. *IEEE Trans. Med. Imag. 29*, 3 (2010), 669–687. 2

© The Eurographics Association 2013.